ENGINEERING TRANSACTIONS • *Engng. Trans.* • **45**, 1, 71–89, 1997
Polish Academy of Sciences • Institute of Fundamental Technological Research
10.2**44**23/engtrans.682.1997

ARCHING ACTION REVISITED

M. JANAS, J. SOKÓŁ-SUPEL and J. SUPEL (WARSZAWA)

Reinforced concrete and elastic-tensionless strips transversally loaded and restrained against longitudinal displacements at supports are considered. The support restraints induce important axial forces and that results in a highly nonlinear and unstable character of the structure response. A commercial FEM code is used and the results are compared with those obtained from an approximate approach based upon the post-yield methodology, proposed years ago by the authors. The latter approach neglects elastic flexural deformations but accounts for axial compliance of the system and furnishes simple analytical expressions for the load vs. displacement relations. It appears from the FEM analysis that the flexural compliance has a negligible impact on the peak-load behaviour. The approximate approach gives satisfactory results, when compliance moduli for the structure and for restraining walls are appropriately chosen. Benchmark cases considered allowed for a proposition concerning determination of these moduli.

1. Introduction

The phenomenon of arching action induces an important rise in the strength of beams and plates restrained against lateral displacements at supports, when the material is "non-symmetric" (with different elastic and/or plastic response to compression and tension). This fact has been well known since many years; however, it is rarely taken into account in the engineering practice. The reason of this reticence is a highly unstable character of the phenomenon; clamped concrete structures under static loads may collapse in an abrupt dynamic manner (see, e.g., [1]).

If the plate supports restrain free longitidinal displacements and if the material is weaker in strength and/or elastic modulus, in tension than in compression, bending under transversal loads is accompanied by important compressive membrane forces. The forces appear from the very beginning of the loading process, whereas the well-known tensile membrane response is negligible until displacements become really large. The compressive forces, when taken into account, provide an important rise in the load-carrying capacity of the structure, in comparison with the results obtained from a purely flexural analysis. The latter

appears, in the case considered, to be kinematically inadmissible. This fact explains a known paradox concerning plastic response of reinforced concrete plates: tests give frequently collapse loads superior to the corresponding upper bounds of the load obtained analytically. This discrepancy cannot be quantitatively explained by the effects of reinforcement hardening and large deflections neglected in the limit analysis.

However, when a consistent limit analysis that satisfies the "internal compatibility" of flexural collapse [2] and accounts for the corresponding axial forces is used, the results strongly overestimate the structure carrying capacity. This is due to the fact that the structure undergoes simultaneous bending and compression and, therefore, its response is very sensitive to geometry changes neglected in the limit analysis. These changes may be accounted for in the framework of an extended limit analysis known as the post-yield approach, [3–6] or by using its version inherent to the deformation theory [1, 7, 8]. In this way, instantaneous collapse loads may be easily obtained plotted against increasing deformation of the structure. However, because of early elastic deformations, the real ultimate peak load is always lower than the initial limit-analysis value obtained for undeformed structure. The rigid-plastic approach cannot determine the deformation at which, in reality, the collapse appears. Therefore, for practical purposes the ultimate-peak load has to be determined as the instantaneous collapse load of the structure deformed up to an assigned displacement value provided by experimental data [8, 9].

The ultimate peak load may be obtained analytically from the post-yield analysis [13], when taking into account only membrane elastic compressibility of the structure and neglecting the corresponding flexural deformations. Unfortunately, a corresponding compliance modulus should be somewhat arbitrarily chosen. In the sixties and early seventies, when the problem was "en vogue", a complete elastic-plastic large-displacement analysis of the problem was practically impossible and approximate approaches were the only way to deal with it.

Taking into account that the unstable structural response is extremely sensitive to the support conditions and material data, reticence of the structural engineers to apply the approximate approaches may be easily understood. However, one can wonder why the effect, whose importance for the structure strength has been confirmed in many experimental studies [8–12], does not attract attention nowadays, when commercial computational FEM codes permit, at least theoretically, to proceed with a complete nonlinear structural analysis. We believe that this reticence results from the uncertainty and complexity concerning determination and introduction of the input data needed in the FEM codes, as well as from random numerical problems accompanying strongly nonlinear FEM analysis. Therefore, it seems necessary to furnish the designer with a tool

enabling him to deal with the discussed problem, with the complexity level comparable to the level of the analysis based on the strength of materials. Therefore, we revisited the problem using our old approach [13] and comparing its results to a nonlinear elastic-plastic incremental simulation using a FEM code [14]. The goal is to evaluate the importance of the flexural deformability neglected in the approximate analysis [13] and to allow for an appropriate choice of the values for the parameters needed in the latter.

The considerations presented here are limited to cases of beams and strips, but the approach may be extended (see [6, 13]) to slabs.

2. Post-yield analysis

The principle of the post-yield approach consists in the use of the limit analysis techniques for determination of instantaneous collapse loads of the structure deformed to a chosen level. In this way a sequence of collapse loads is obtained, which – when plotted against a reference displacement – describes a load-deflection curve of the quasi-static structure response. This post-yield curve characterizes geometrical hardening (or softening) of the structure. The collapse mode describing the deformed configuration of the structure may be either a continuation of the incipient plastic flow or, if automatic procedures are used (e.g., in [15]), it may be updated at each step of the deformation process. Hence, the deformation described by a sequence of collapse modes, is dependent exclusively on purely plastic deformation.

Such an approach, neglecting the contribution of elastic deformation to configuration changes, can describe relatively well the advanced deformation processes, when elastic strains are negligible in comparison with the plastic ones. In an early phase of the process, elastic deformation may be of the same order or more important than the purely plastic one. However, in the early phase the changes of configuration due to deformation are, in most cases, of small importance. Therefore, the rigid-plastic model is acceptable in both the cases. This approach using, as follows from the limit analysis theory, the associated plastic flow rule, was applied to many structural cases, e.g., to plates [4–6, 16] and frames [17]. It was also generalized to the analysis of inadaptation processes [18]. A conceptually identical approach but using a deformation-type plastic theory instead of the flow rule, was applied to concrete-oriented analyses [1, 7–9].

Unfortunately, the rigid-plastic post-yield approach appears to be unsatisfactory in the case of an unstable structure behaviour at the early phase of the deformation. For example, elastic deformations contribute considerably to the nonlinear character of the response for slender structures undergoing simulta-

neous bending and axial compression. This is, namely, the case of structures built of a material with different yield points in compression and tension. Important compressive axial forces appear from the very beginning of the deformation process, when such a structure undergoes bending under transversal loads and support restraints prevent free longitudinal displacements. To visualize the importance of this effect, load-deflection curves are given in Fig. 1 a for a clamped weakly reinforced concrete strip (Fig. 2) loaded by a concentrated force at the midspan. The results concern the cases of restrained and free longitudinal displacements at supports. They are obtained from an incremental FEM simulation using elastic-perfectly plastic tensionless model for the concrete. Details on the FEM analysis are given in the next section. The rigid-plastic curve obtained from the post-yield analysis in the case of restrained supports will commence with the maximum value at zero deflection and will strongly differ, at the early stage, from the real curve. In the case of free longitudinal displacements at supports, the influence of the initial geometrical nonlinearity is indiscernible and the rigid-plastic model represents well the response. The early phase of the response is given in details in Fig. 1 b to show that the restrained strip is significantly more rigid in the elastic (but nonlinear because of the tensionless response of the concrete) and in the elastic-plastic phases than the unrestrained strip.

To avoid errors induced in the early phase by the rigid-plastic model, elastic deformations must be accounted for in some manner. The compressive axial force is responsible for the unstable character of the structure response and the evolution of this force depends upon the elastic compliance in the longitudinal direction. Therefore, this compliance should be necessarily taken into account. On the other hand, elastic deformations corresponding to curvature changes in elastic and elastic-plastic zones do not influence qualitatively the structure behaviour. These observations became a basis of an approximate method for the analysis of the arching-action behaviour [13]. This approach neglecting flexural elastic-plastic deformations may be applied in the framework of the post-yield methodology. A similar approach was applied later to circular plates with partial fixity [19] and to the punching analysis of concrete slabs [20]. We recall below its main results, following [13]. For sake of self-consistency of the paper, details on the assumptions and the procedure are recalled in the Appendix.

The example used to illustrate the method is a clamped centrally loaded strip (Fig. 2) of span L and height of the cross-section h. It is built of a tensionless elastic-perfectly plastic material with the yield stress σ_c. Reinforcement layers of the area A and the yield stress σ_s may be posed at one or two external faces of the cross-section.

Elastic compliance in the longitudinal direction of the support and of the strip is modeled by appropriate springs shown in Fig. 2; the support-spring model is

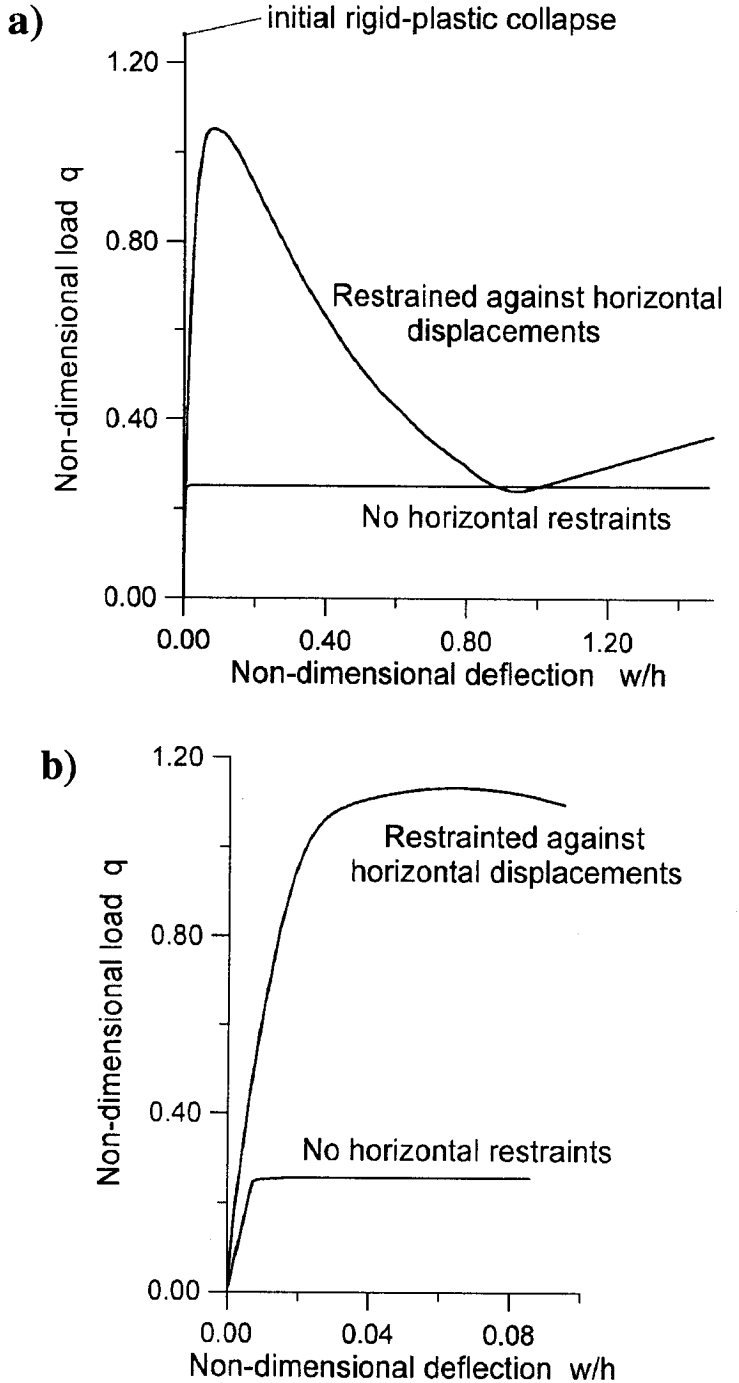

FIG. 1. Load-deflection curves obtained from the incremental FEM analysis for a clamped, symmetrically reinforced concrete strip with a span-to-thickness ratio $L/h = 14$.

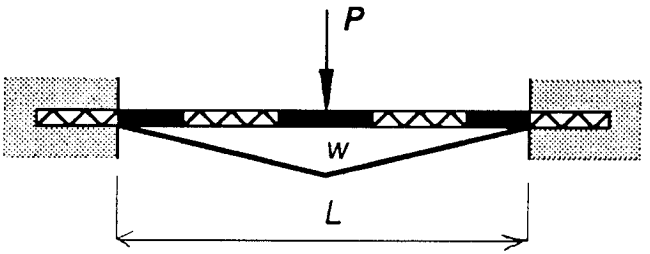

FIG. 2. Clamped strip with the collapse mode assumed in the post-yield analysis; elastic compliance is modeled by springs.

exact, whereas the strip spring represents only a reduced average compliance of the entire structure. Depending upon the modulus of the springs, the approach may cover all the cases: from the unrestrained supports to the purely rigid-plastic post-yield behaviour.

Following the rigid-plastic model of the post-yield approach, the instantaneous collapse mode of the structure consists of rigid-body rotations around the supports (Fig. 2) and, therefore, plastic deformations appear only at the central and support plastic hinges. Kinematical compatibility of the plastic flow of the deformed structure needs the instantaneous relative rotation axes in all the hinges lying in one horizontal plane. Position of this plane, together with a relation for the elastic shortening rate of the strip, determine positions of neutral axes for the generalized plastic strain rates; following the plastic flow law, they coincide with neutral axes for normal stresses. Equilibrium of the stresses gives a linear differential equation for the axial force N with respect to the central deflection w. Its solution, together with unstressed initial conditions ($w = 0$, $N = 0$), describes the evolution of the non-dimensional force $n = N/N_0$ as a function of the current non-dimensional central deflection $\alpha = w/h$:

$$n = (1 - e^{\varepsilon\alpha})\left(k + \frac{1}{\varepsilon}\right) - \alpha. \tag{1}$$

The reduced elastic compliance ratio ε is:

$$\varepsilon = \frac{8Eh^2}{\sigma_c L^2} \tag{2}$$

and k describes plastic characteristics of the cross-section. For a tensionless singly reinforced and for a doubly reinforced symmetrical cross-sections, respectively, k is expressed as follows:

$$k = 1 - \eta_b - \eta_t, \qquad k = 1 \tag{3}$$

with η_b, η_t representing intensities of the bottom (central hinge) and top (support) reinforcement, respectively:

$$\eta = \frac{A\sigma_s}{h\sigma_c}. \tag{4}$$

The plastic moduli of the cross-section are:

$$M_0 = \frac{\sigma_c h^2}{8}, \qquad N_0 = \frac{\sigma_c h}{2}. \tag{5}$$

When the value of the axial force (1) is introduced to the equation of the limit equilibrium of the structure, one obtains the relation for the load-deflection curve looked for,

$$q = \frac{PL}{8M_0} = q_Y + (k-\alpha)^2 - \left[k - (1 - e^{\varepsilon\alpha})\left(k + \frac{1}{\varepsilon}\right)\right]^2. \tag{6}$$

The non-dimensional collapse load q_Y corresponds to simple bending with free horizontal displacements, i.e. in absence of the axial forces. The curves (6) for different compliance ratios ε are given in Fig. 3. The case $\varepsilon = 0$ represents the purely flexural response, and $\varepsilon \to \infty$ the rigid-plastic model. For an advanced deformation process a pure membrane response appears, corresponding to the

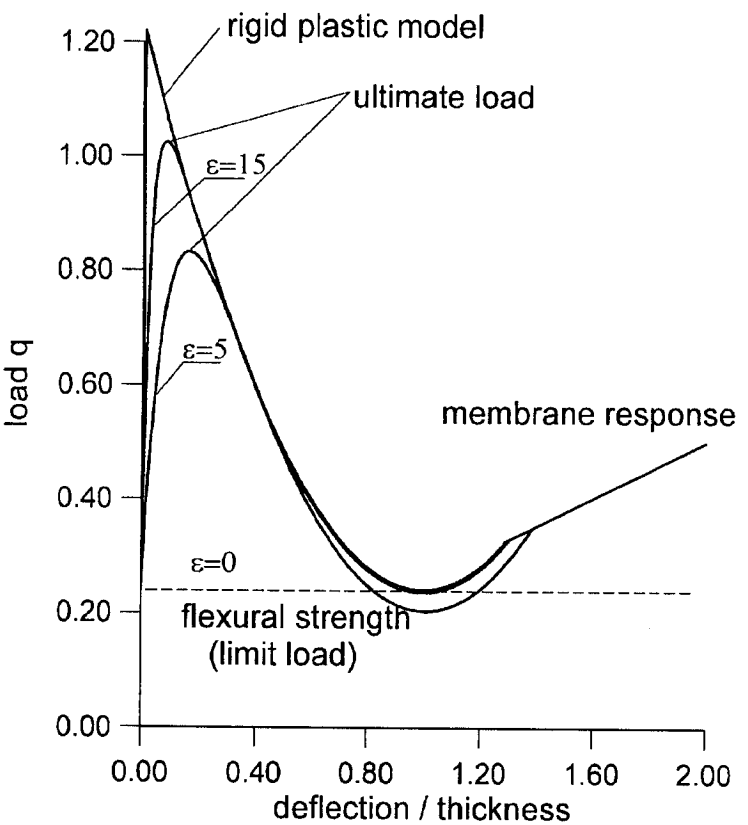

FIG. 3. Approximate load-deflection analytical curves (6) for the strips with different compliance ratios.

straight part of the plot. The membrane response is, of course, independent of the elastic characteristics of the structure. A small intermediate phase is neglected for the sake of simplicity.

The above results are directly applicable also to other symmetric loading cases of the clamped strip.

It is obvious that the ratio ε is only a conventional representation of the average longitudinal compliance of the strip. In reality this compliance depends upon the moment-to-force ratio M/N and, therefore, is variable along the strip axis. It was proposed in [13], following some observations concerning test results, to determine the value of ε by using a reduced Hooke modulus E equal to one half of the nominal modulus of the material at compression.

Since the results, and especially the peak-load value depend very strongly upon the choice of the compliance ratio, its values should be assumed on the basis of a more exact analysis.

3. FEM INCREMENTAL ANALYSIS

The incremental FEM analysis was conducted using the ABAQUS program [14]. Calculations were performed on the CRAY CS-6400 belonging to the Computer Center of the Warsaw University of Technology.

To allow for a quantitative comparison of the results of the FEM analysis with the results of the discussed above approximate approach [13], the same constitutive material model is adopted in both cases. This concerns the elastic-perfectly plastic tensionless material of the strip core and perfectly thin elastic-plastic reinforcement layers uniaxially stressed. Tangential stresses being disregarded, as in the classical Bernoulli beam theory, the core material is considered to yield under uniaxial stress. Therefore, the associated plastic flow rule implies the coincidence of the sign of axial stresses with that of the plastic strain rate. This remark is important, because in the post-yield approach applied to concrete structures the coincidence concerns the signs of stresses and strains (a deformation-type theory).

The influence of a tensile strength of the concrete σ_t neglected in the above model was evaluated in the case of unreinforced cross-section, where it should be relatively most significant. The concrete behaviour in compression is, as before, elastic-perfectly plastic. In tension it is elastic up to the peak tensile strength $\sigma_t = 0.09\sigma_c$ followed by a linear softening until zero strength at the full crack opening. To avoid a mesh-sensitivity of such a model, the Hilleborg softening criterion is adopted, with the full crack opening of 0.05 mm smeared along one element length. This influence is shown in Fig. 4; it practically disappears well

before the phase near the ultimate load, which is of principal practical interest. Therefore, in the main part of the study the concrete is assumed to be tensionless.

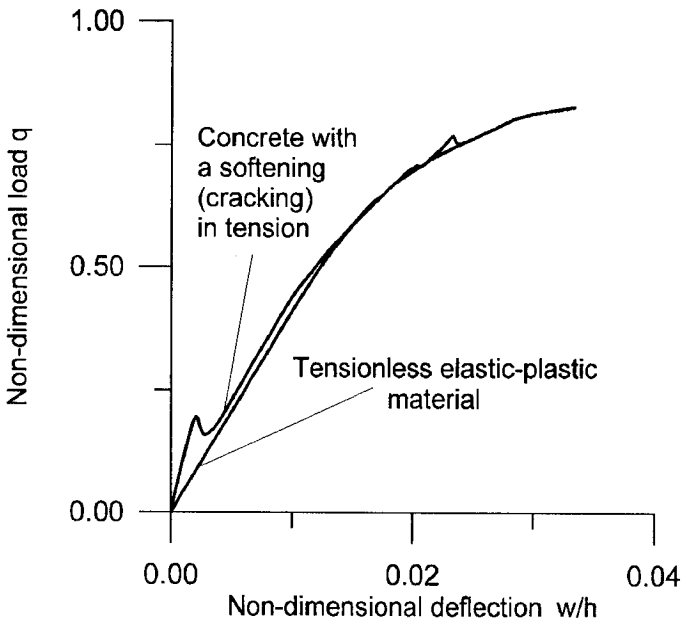

FIG. 4. Early stage of unreinforced elastic-perfectly plastic strip with and without a limited tensile strength and ductility of the concrete accounted for; incremental analysis.

The finite elements used are standard plane beam elements B21 from the Abaqus [14] catalogue. These were 2-node linear elements with uniaxial reinforcement layers. Because of the particular character of the tensionless response, the number of integration points across the thickness had to be remarkably larger than that normally recommended.

The incremental equilibrium equations were based on the small-strain large-displacements and large-rotations beam theory. They were integrated, following a standard Abaqus algorithm, using the Newton method. The procedure was displacement-controlled and was continued up to the state of advanced tension membrane response. Nevertheless, the main interest, and the more precise results concern the early phase of the structure response, in the vicinity of the ultimate peak load.

Calculations started from a reference case of the clamped strip shown in Fig. 2 with the characteristic data: the strip span $L = 300\,\text{cm}$, the cross-section height $h = 30\,\text{cm}$, the concrete modulus $E = 30\,\text{GPa}$ and its compressive strength $\sigma_c = 40\,\text{MPa}$; reinforcement steel: $E = 210\,\text{GPa}$, $\sigma_s = 250\,\text{MPa}$. Then, the parametric study concerned the span-to-height ratio $L/h = 7 - 35$ and the concrete modulus-to-strength ratio $E/\sigma_c = 250 - 2250$. Reinforcement intensity was taken

from 0% up to 1.6% for each reinforcement layer; the layers were supposed to coincide with external faces of the strip; they were posed either symmetrically or only at the face undergoing extension.

Results of the incremental analysis confirm that the approximate approach neglecting flexural elastic-plastic deformation may represent qualitatively correctly the real response of the elastic-perfectly plastic structures. The approximate load-deflection curve commences at $w = 0$ with the load value equal to the flexural carrying-capacity q_Y, but the real curve climbs very steeply (at least two times faster than in pure bending, see Fig. 1 b) and attains this load at deflection less than 1% of the strip thickness. Therefore, the difference of the two curves is nearly indiscernible in this very early phase. The rise in the instantaneous collapse load of the deformed structure is due to the increase of the axial force. However, the maximum load is attained at a deflection less than 10% of the thickness, well before the axial force attains its maximum. Then, the supportable load that may maintain the structure in the inertia-free equilibrium must decrease, but the curve slope is significantly less steep than at its ascending part. If the load remains unchanged after it attains the maximum, the structure snaps-through in a dynamic way until the horizontal load-deflection path meets the ascending branch of the curve. This problem was dealt with using the approximate approach in [21].

Since the incremental procedure was displacement-controlled, the standard algorithm dealt easily with the instability zone at the peak-load. Some problems occur in certain cases at the minimum-point load, especially for the cases of single and/or discontinuous reinforcement. In the rigid-plastic model the minimum of the curve is strictly equal to the purely flexural load-carrying capacity and corresponds to the zero axial force. Due to elastic deformations, this minimum load is slightly inferior to the flexural value. For very compliant structures this difference may be remarkable. At the following ascending branch, the axial force attains the tensile strength in the weaker of the plastic hinges. Then, a membrane response is continued, represented by a linear load-deflection relation. Its beginning for symmetrical reinforcement is shown in Fig. 6 a. For single reinforcement this response is attained at a more advanced deformation.

When a series of structures are considered with various L/h and E/σ_c ratios but chosen in such a way that the compliance ε (Eq. (2)) remains constant, the load-deflection curves are practically identical. For unreinforced and symmetrically reinforced structures, the coincidence is so exact that the authors suspect that the kernels of the solution of the nonlinear differential equation governing the problem depend exclusively on this parameter. Therefore, the presented cases differ only in the reinforcement (type and intensity η) and in the compliance ε. The same parameters η and ε are the only ones that influence the approximate

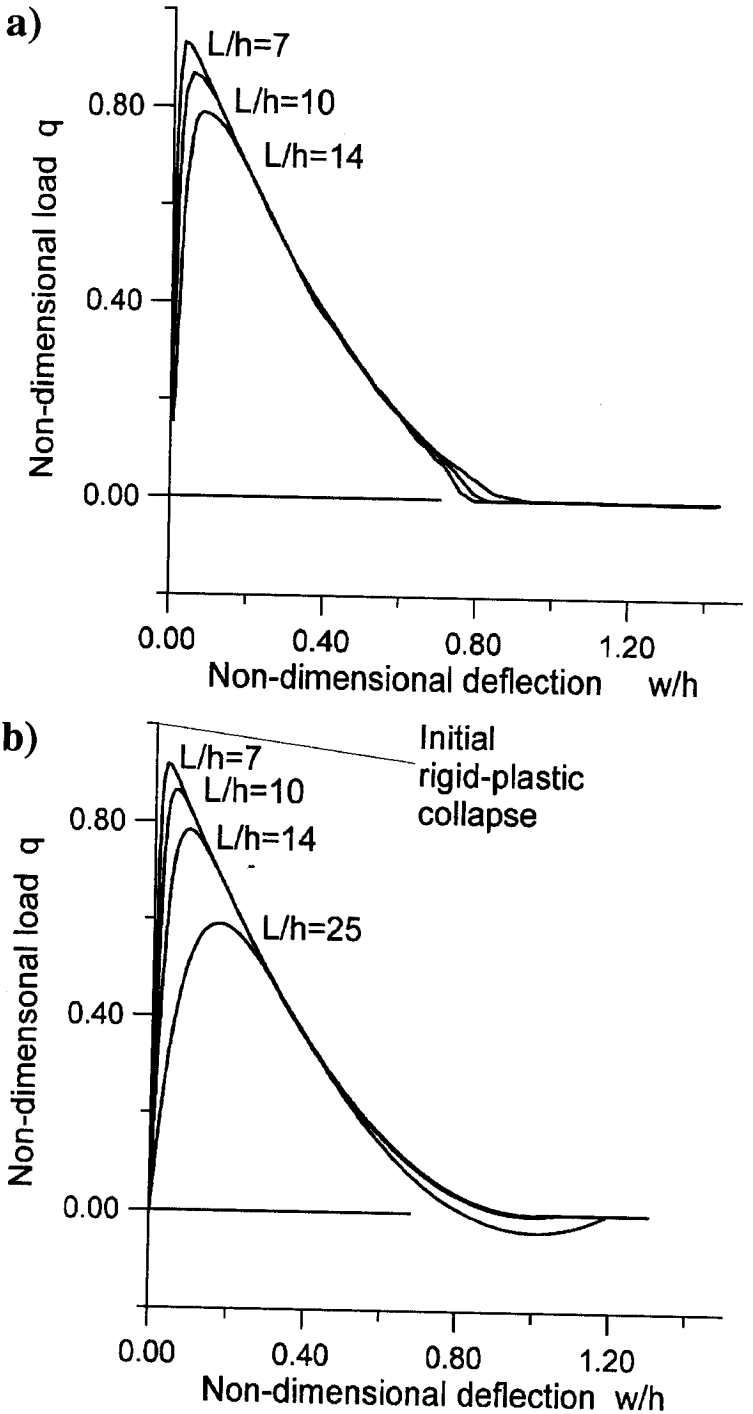
a)
L/h=7
L/h=10
L/h=14
0.80
0.40
0.00
Non-dimensional load q
0.00
0.40
0.80
1.20
Non-dimensional deflection w/h
b)
Initial
rigid-plastic
collapse
L/h=7
L/h=10
L/h=14
L/h=25
0.80
0.40
0.00
Non-dimensonal load q
0.00
0.40
0.80
1.20
Non-dimensional deflection w/h

[FIG. 5]

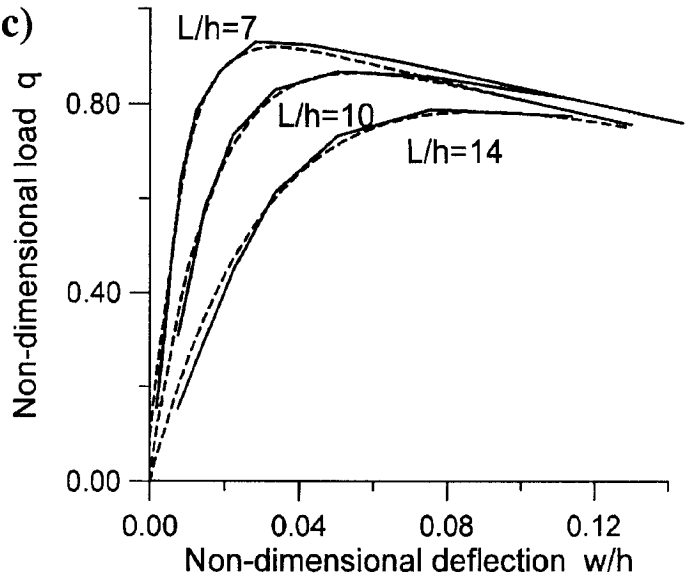

FIG. 5. Unreinforced elastic-plastic tensionless strip: a) incremental FEM analysis; b) approximate analytical results (6); c) early stage – comparison of the FEM (solid curves) and analytical (dashed curves) results for different slenderness ratios.

solution. This fact simplifies a quantitative comparison of both the approaches. The curves are identified in the presented diagrams by the value of the L/h ratio, whereas the corresponding material reference ratio is always $E/\sigma_c = 750$. The non-dimensional form of the load in the figures is taken following Eq. (6).

The values of ε used in the approximate solution (6) for the comparison with the FEM results are calculated with the Hooke modulus E equal one half of the concrete modulus in compression. In the case of unreinforced strips (Figs. 5), the results following (6) coincide so perfectly with the numerical data that the difference is discernible only in the detail of the early response (Fig. 5 c). In the presence of the reinforcement (Figs. 6) the fit would be better if the reduced modulus was taken slightly larger.

Evolution of the axial force for unreinforced and symmetrically reinforced strips is given in Fig. 7, following the incremental and the approximate analytical solutions. Symmetrical reinforcement does not influence results of the analytical approach, whereas its influence on the FEM results is practically negligible. Since the approximate approach represents well the axial force evolution, it may simulate properly the unstable character of the response, this character being induced by the presence of the compressive force.

Only one curve concerning the case of non-symmetric reinforcement is given in Fig. 8. It concerns the reinforcement of the same intensity put on all the faces undergoing extension. The response is qualitatively the same as in the case of

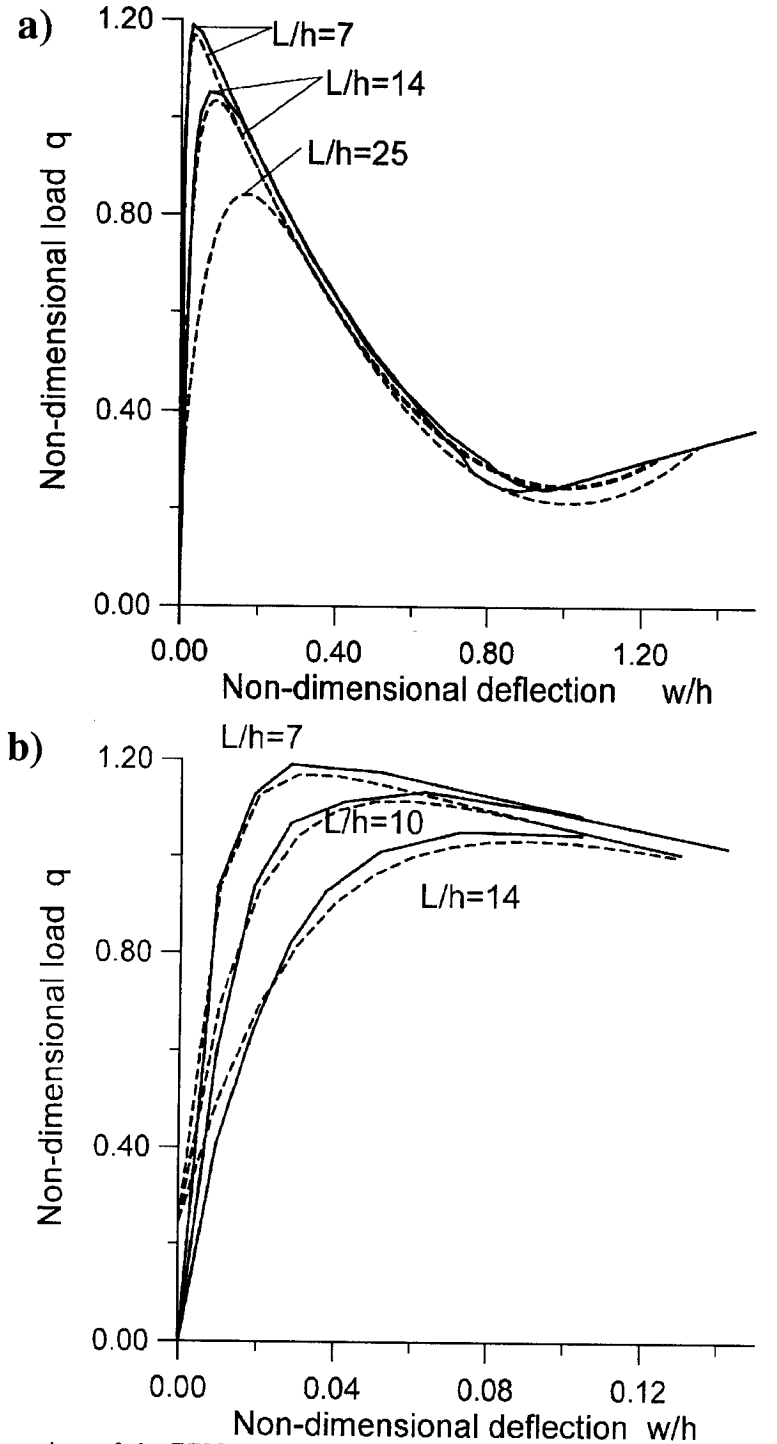

FIG. 6. Comparison of the FEM and analytical results for the strip with a double symmetric reinforcement (0.5% for each layer): a) the whole curve, b) the early stage.

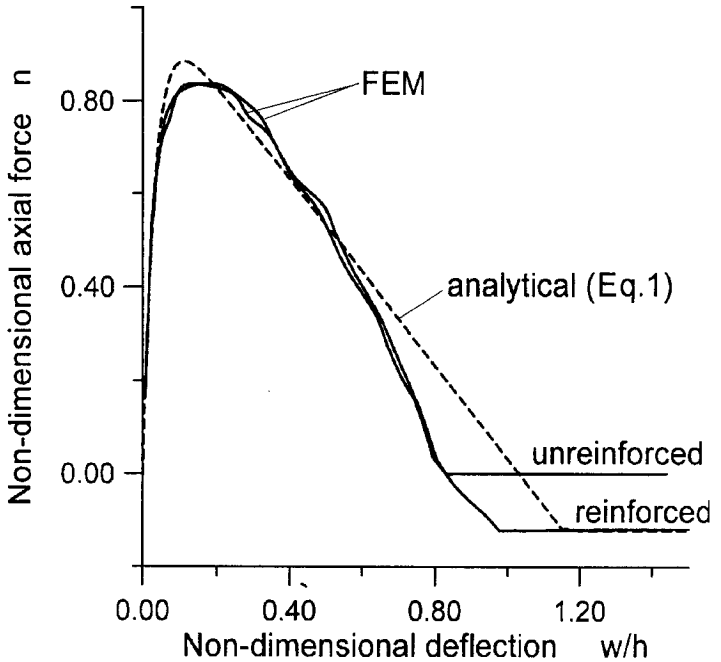

FIG. 7. Evolution of the axial force for the unreinforced (the case following Fig. 5) and reinforced (following Fig. 6) strip: FEM (solid lines) and analytical (dashed line) results.

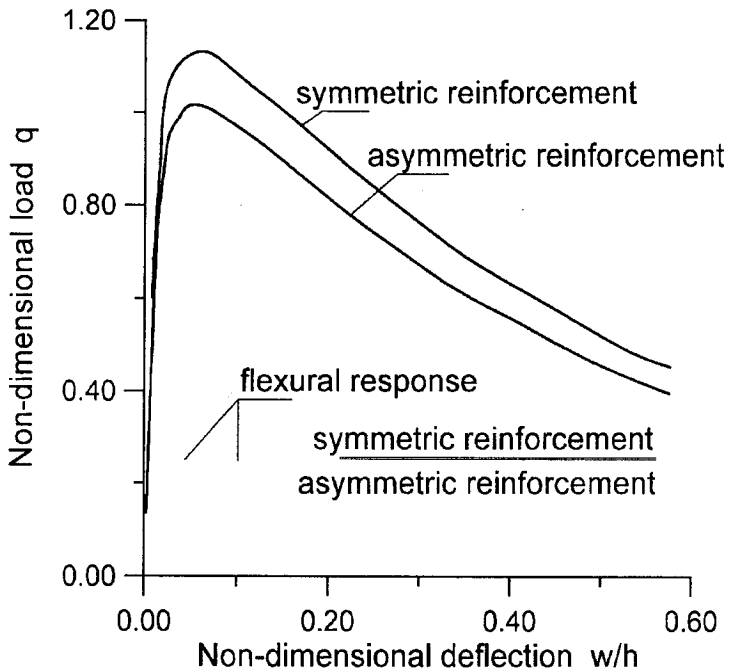

FIG. 8. Load-deflection curves for a symmetric double reinforcement and for a single reinforcement on the face undergoing extension (0.5% reinforcement for each layer).

symmetric reinforcement, following both the incremental and the approximate analysis. Conclusions concerning the choice of the reduced modulus E in the approximate approach needed for the best coincidence of its results with the numerical data are the same as those for symmetric reinforcement. The compressed reinforcement seems to have no influence on this choice. It may be interesting to observe that the influence of the compressed reinforcement on the ultimate peak-load is significantly more important than its influence on the purely flexural strength of the structures.

4. Conclusions

The incremental FEM analysis (using the ABAQUS code [14]) for longitudinally restrained clamped strips shows that flexural deformations have a negligible effect on the geometrically nonlinear behaviour of the structure. That concerns, first of all, the phase near the ultimate peak load, when this nonlinearity is of essential importance. That is why the approximate approach [13] based on the post-yield rigid-plastic model but accounting for an elastic longitudinal compliance of the strip (and/or of its supports) may simulate well, at least qualitatively, the real response of elastic-perfectly plastic tensionless structures.

It appears (maybe that it is obvious, but not for the authors) that, even in the large-deformation range, the elastic-perfectly plastic response of beams is a function of only one parameter ε (Eq. (2)) representing the elastic compliance of the structure. The response of the structures with different characteristics (L/h and E/σ_c ratios) will be the same if the parameter ε remains constant. The same situation occurs in the approximate analysis.

To obtain the best coincidence of the approximate results with the results of the complete incremental analysis, the parameter ε used in the former approach should be calculated using the modulus E equal to one half of the concrete Hooke modulus in compression E_c. For stronger reinforcement, a little better fit will be obtained if the value of E used is slightly larger, i.e., if:

$$E = E_c(1 + 8\eta)/2. \tag{8}$$

The symbol η stands for an average intensity (4) of the reinforcement in the tensile zones of the plastic hinges.

Using the above results, the simple formulae (of the complexity level similar to the level in the strength of materials) may be proposed accounting for the arching action, in spite of an unstable character of the response. However, a more extensive parametric study is needed to obtain reliable results. The same concerns extrapolation of the above conclusions to two-way RC slabs.

APPENDIX. APPROXIMATE ELASTIC-PLASTIC POST-YIELD APPROACH [13]

To ensure kinematical admissibility of the instantaneous plastic flow of the strip deformed following the plastic collapse mode (Fig. 2), displacement velocities have to be determined by the rigid-body rotation rule. Generalized strain rates in the plastic hinge are equal to displacement rate discontinuities of the adjacent rigid bodies. In the case of the rigid-plastic model assumed in the classical post-yield analysis, the discontinuities are described by the vectors of relative rotation rates. If elastic longitudinal compressibility of the strip is accounted for, a longitudinal displacement rate proportional to the rate of the axial force evolution has to be added. Because of the symmetry of the system, axes of the rotation vectors lie in one horizontal plane (points O_n and O_p in Fig. 9) at a distance z from the middle plane at supports.

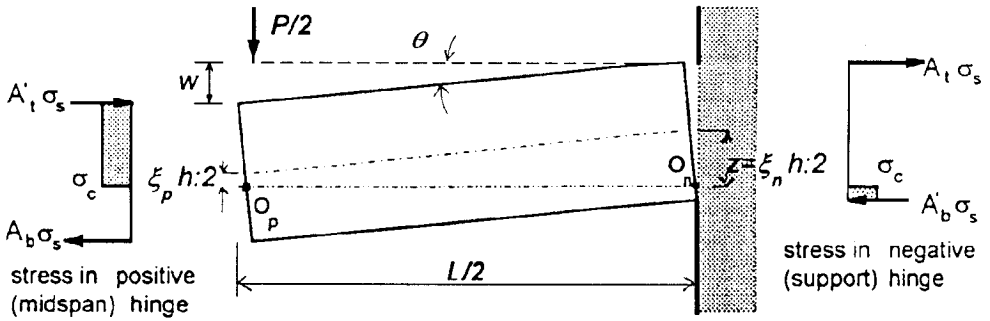

FIG. 9. A half-span of a clamped reinforced concrete strip; instantaneous plastic flow at finite deflection w.

Extension rate of the middle plane $\dot{\lambda}$ and the curvature rate $\dot{\kappa}$ in the hinges are determined by the rotation rate $\dot{\Theta}$ around the supports

$$\begin{aligned} \dot{\lambda}_n &= \dot{\Theta} z, & \dot{\kappa}_n &= -\dot{\Theta}, \\ \dot{\lambda}_p &= -2\dot{\Theta}(z-w) + \lambda_e, & \dot{\kappa}_p &= 2\dot{\Theta}, \end{aligned} \tag{A.1}$$

with the subscripts n and p denoting the negative (support) and positive (midspan) hinges, respectively. The dot denotes differentiation with respect to a time-like kinematical parameter. The elastic shortening rate of the strip $\dot{\lambda}_e$ is proportional to variation of the axial force N:

$$d\lambda_e = \frac{L}{Eh} dN. \tag{A.2}$$

Dimensionless positions ξ of the instantaneous neutral axes for strain rates and for stresses in the plastic hinges are

$$\xi = -\frac{2\dot{\lambda}}{h\dot{\kappa}} \tag{A.3}$$

and a relation between these positions may be obtained from Eqs. (A.1). Using non-dimensional quantities following Sec. 2, this relation may be written as:

$$\xi_p = \xi_n - 2\alpha - \frac{2}{\varepsilon}\frac{dn}{d\alpha}. \tag{A.4}$$

Yield criteria for the cross-section may be expressed, following the stress diagrams given in Fig. 9, in a parametric form:

$$\begin{aligned} m_p &= 1 - \xi_p^2 + 4(\eta_b + \eta_t'), & n_p &= 1 + \xi_p - 2(\eta_b - \eta_t'), & \dot{\kappa} &> 0, \\ m_n &= -1 + \xi_n^2 - 4(\eta_t + \eta_b'), & n_n &= 1 - \xi_n - 2(\eta_t - \eta_b'), & \dot{\kappa} &< 0, \end{aligned} \tag{A.5}$$

where η denotes intensity of a reinforcement layer following Eq. (4), subscripts b, t concern bottom and top layers, respectively, and η' indicates compressed reinforcement (top in the positive hinge and bottom in the negative one).

In the absence of horizontal external loads, the axial force is constant along the strip and the condition $n_n = n_p$ gives, together with Eqs. (A.4), (A.5), the following differential equation

$$\frac{1}{\varepsilon}\frac{dn}{d\alpha} + n = k - \alpha, \tag{A.6}$$

where the parameter k is

$$k = 1 - \eta_b - \eta_t + \eta_b' + \eta_t'. \tag{A.7}$$

Solution of Eq. (A.6), gives, together with the initial condition $\alpha = 0$, $N = 0$, expression for the axial force:

$$n = (1 - e^{\varepsilon\alpha})\left(k + \frac{1}{\varepsilon}\right) - \alpha. \tag{A.8}$$

Equation of the limit equilibrium of one half of the strip

$$\frac{PL}{4M_0} - m_p + m_n + 4n\alpha = 0 \tag{A.9}$$

gives, together with Eqs. (A.5) and (A.8), expression for a current instantaneous limit load of the deformed structure. It describes the load-deflection curve of the quasi-static response, plotting the non-dimensional load q versus the non-dimensional central deflection $\alpha = w/h$:

$$q = \frac{PL}{8M_0} = q_Y + (k - \alpha)^2 - \left[k - (1 - e^{\varepsilon\alpha})\left(k + \frac{1}{\varepsilon}\right)\right]^2. \tag{A.10}$$

The non-dimensional limit load q_Y for the longitudinally unrestrained structure ($N = 0$) is equal to:

$$q_Y = 4(\eta_b + \eta_t) + 2(\eta_t - \eta_b')^2 + 2(\eta_b - \eta_t')^2. \tag{A.11}$$

The form given above concerns the case when the compressed reinforcement in the cross-section is not stronger than reinforcement in the tension zone.

When the axial force attains its maximum admissible value in the weaker hinge, further process is continued with constant stress resultants. Its results coincide with the rigid-plastic membrane response. Since our main interest concerns the phase of the ultimate peak-load, only the results for two particular cases are given here: for a single reinforcement ($\eta_b = \eta_t = \eta$, $\eta' = 0$)

$$q = 8\eta + 4\eta(\alpha - 1), \tag{A.12}$$

and for a double symmetric reinforcement ($\eta_b = \eta_t = \eta_b' = \eta_t' = \eta$):

$$q = 8\eta. \tag{A.13}$$

The membrane response may be preceded by an intermediate phase. This phase may be of non-negligible extent if the elastic compliance in the overall tension significantly exceeds the compliance of the structure under axial compression (see [13]). This problem will not be discussed here because of the reason given above.

REFERENCES

1. R.H. WOOD, *Plastic and elastic design of plates*, Thames and Hudson, London 1961.
2. M. JANAS, *Kinematical compatibility problems in yield-line theory*, Mag. Concrete Res., **19**, 33–44, 1967.
3. R. M. HAYTHORNTHWAITE, *Beams with full end fixity*, Engineering, **183**, 110–112, 1957.
4. C.T. MORLEY, *Yield-line theory for reinforced concrete slabs at moderately large deflections*, Mag. Concrete Res., **19**, 61, 211–222, 1967.
5. C.R. CALLADINE, *Simple ideas in the large-deflection plastic theory of plates and slabs*, [in:] Engineering Plasticity, 93–127, J. HEYMAN, F.A. LECKIE [Eds.], Cambridge Univ. Press, London 1968.
6. M. JANAS, *Large plastic deformations of reinforced concrete slabs*, Int. J. Solids Struct., **4**, 61–74, 1968.
7. A. SAWCZUK and L. WINNICKI, *Plastic behaviour of simply supported concrete plates at moderately large deflexions*, Int. J. Solids Struct., **1**, 97, 1965.
8. R. PARK, *Reinforced concrete slabs*, J. Wiley, New York 1980.
9. A. JACOBSON, *Membrane-flexural failure modes of restrained slabs*, J. Struct. Div. ASCE, **93**, 85–112, 1967.
10. K.P. CHRISTIANSEN, *The effect of membrane stresses on the ultimate strength of the interior panel of a reinforced concrete slab*, The Structural Engng., **41**, 261–165, 1963.
11. E.H. ROBERTS, *Load-carrying capacity of slab-strips restrained against longitudinal expansion*, Concrete, **3**, 369–378, 1969.

12. S.S.J. MOY and B. MAYFIELD, *Load-deflection characteristics of rectangular reinforced concrete slabs*, Mag. Concrete Res., **24**, 209–218, 1972.

13. M. JANAS, *Arching action in elastic-plastic plates*, J. Struct. Mech., **1**, 277–293, 1973.

14. *Abaqus*, Version 5.4, Hibbitt-Karlsson-Sorensen Inc., 1994.

15. H.B. BONDOK, M. JANAS and A. SIEMASZKO, *A numerical program for post-yield and inadaptation analysis of space skeletal structures*, Proc. Polish. Conf. Computational, Mechanics, 129–137, W. GILEWSKI [Ed.], Publ. Politech. Świętokrzyska, Kielce 1993.

16. M.W. BRAESTRUP, *Dome effect in RC slabs: rigid-plastic analysis*, J. Struct. Div. ASCE, **106**, 1237–1253, 1980.

17. M.K. DUSZEK and A. SAWCZUK, *Stable and unstable states of rigid-plastic frames at the yield-point load*, J. Struct. Mech., **4**, 33–47, 1976.

18. A. SIEMASZKO and J.A. KOENIG, *Analysis of stability of incremental collapse of skeletal structures*, J. Struct. Mech., **13**, 301–321, 1985.

19. M.W. BRAESTRUP and C.T. MORLEY, *Dome effect in reinforced concrete slabs: elastic-plastic analysis*, J. Struct. Div. Proc. ASCE, **106**, 1255, 1980.

20. J.S. KUANG and C.T. MORLEY, *A plasticity model for punching shear of laterally restrained slabs with compressive membrane action*, Int. J. Mech. Sci, **35**, 371–385, 1993.

21. M. JANAS, *Snap-through in RC beams under transversal loads* [in Polish], IFTR Reports, Nr. 32, 1975.

POLISH ACADEMY OF SCIENCES
INSTITUTE OF FUNDAMENTAL TECHNOLOGICAL RESEARCH.

e-mail: mjanas@ippt.gov.pl
e-mail: jsokols@ippt.gov.pl
e-mail: jsupel@ippt.gov.pl

Received December 5, 1996.

ENGINEERING TRANSACTIONS • Engng. Trans. • **45**, 2, 327, 1997
Polish Academy of Sciences • Institute of Fundamental Technological Research

E R R A T U M

ARCHING ACTION REVISITED

M. JANAS, J. SOKÓŁ-SUPEL and J. SUPEL (WARSZAWA)

Engineering Transaction, **45**, 1, 71–89, 1997

formula	is	should be
(1), (6), (A.8), (A.10)	$e^{\varepsilon\alpha}$	$e^{-\varepsilon\alpha}$
(A.11)	$4(\eta_b+\eta_t)+2(\eta_t-\eta_b')^2+2(\eta_b-\eta_t')^2$	$4(\eta_b+\eta_t)-2(\eta_t-\eta_b')^2-2(\eta_b-\eta_t')^2$